



Published in final edited form as:

Anal Methods. 2020 January 21; 12(3): 272–280. doi:10.1039/c9ay02247c.

A multicolor multiplex lateral flow assay for high-sensitivity analyte detection using persistent luminescent nanophosphors†

Adheesha N. Danthanarayana^a, Erin Finley^a, Binh Vu^b, Katerina Kourentzi^b, Richard C. Willson^{b,c,d}, Jakoah Brgoch^a

^aDepartment of Chemistry, University of Houston, Houston, Texas 77204, USA.

^bDepartment of Chemical and Biomolecular Engineering, University of Houston, Houston, Texas 77204, USA.

^cDepartment of Biology and Biochemistry, University of Houston, Houston, Texas 77204, USA

^dEscuela de Medicina y Ciencias de Salud, Tecnológico de Monterrey, Monterrey, Nuevo León 64710, Mexico

Abstract

Incorporating two persistent luminescent nanophosphors (PLNPs), green-emitting $\text{SrAl}_2\text{O}_4:\text{Eu}^{2+},\text{Dy}^{3+}$ (SAO) and blue-emitting $(\text{Sr}_{0.625}\text{Ba}_{0.375})_2\text{MgSi}_2\text{O}_7:\text{Eu}^{2+},\text{Dy}^{3+}$ (SBMSO), in a single lateral flow assay (LFA) establishes a luminescence-based, multiplex point-of-need test capable of simultaneously detecting two different analytes in a single sample. The advantages of this system are the high sensitivity and photostability of PLNPs, while only requiring access to minimal hardware and a smartphone for signal detection. The PLNPs were obtained by first wet milling bulk synthesized phosphor powders, followed by fractionation using differential centrifugal sedimentation to obtain monodisperse nanoparticles. A modified Stöber process was then employed to encapsulate the nanoparticles in a water-stable silica shell followed by attaching antibodies to the particles' surfaces using reductive amination chemistry. The resulting PLNPs were incorporated in an LFA to concurrently detect two independent model analytes, prostate-specific antigen (PSA) and human chorionic gonadotropin (hCG). The multicolor-multiplex PLNP-based assays were finally imaged using a smartphone-based imaging system with excellent detection limits (0.1 ng mL^{-1} of PSA and 1 ng mL^{-1} of hCG) that are competitive with commercially available LFAs.

1. Introduction

Point-of-need testing is a critical and ever-growing research area in the medical and biotechnological fields. It provides significant advantages to healthcare providers by allowing immediate and convenient testing in low resource settings such as less-developed countries or a patient's home. Indeed, these tests allow quicker clinical decisions without the

†Electronic supplementary information (ESI) available. See DOI: 10.1039/c9ay02247c

jbrgoch@uh.edu; willson@uh.edu.

Conflicts of interest

The authors declare no competing financial interest.

need for sophisticated and expensive instrumentation or highly trained personnel.^{1–3} Among point-of-need testing methods, lateral flow assays (LFAs) have gained significant attention because of their simplicity, low cost, and user-friendly format.^{4–6} LFAs are wicking-membrane-based devices (the components are shown in Fig. 1) that can conduct an immunoassay for a target analyte in a liquid sample based on the biorecognition between antigen and antibody. When the sample containing the analyte (antigen) is applied onto the sample pad, it first migrates to the conjugate pad where it binds to analyte-specific antibodies that have been conjugated to reporter labels. The resulting analyte–antibody–label complex then continues to flow along the porous LFA membrane where another antibody that is primary to the analyte, captures this complex at a test line. The sandwich binding of the labeled and primary antibodies mediated by the presence of the analyte produces a response, typically as simple as the appearance of a color, at the test line that indicates the presence of the analyte in the sample. Any excess labeled antibody is finally captured by secondary antibodies at the control line indicating the proper liquid flow through the strip.^{3,5,6}

For given antibodies, the test sensitivity primarily depends on the detectability of the reporter. Some commonly used reporters are gold nanoparticles, colored latex nanobeads, organic fluorophores, and quantum dots.^{5–8} Gold nanoparticles are the most commonly used reporters due to their ease of functionalization, size-tunable optical properties, and excellent chemical stability.⁵ Colored latex beads are also easy to functionalize, and they are available at a relatively low cost.⁸ Organic fluorophores show enhanced sensitivity while quantum dots show resistance to photobleaching and they have unique size-tunable optical properties.^{5,8} Unfortunately, there are drawbacks for each of these reporters. For example, gold nanoparticles and colored latex beads have limited sensitivity because they are colorimetric methods.^{9,10} Fluorophores and quantum dots exhibit better sensitivity than gold nanoparticles and colored latex beads;^{11,12} however, fluorophores are not photostable^{5,13} and quantum dots are costly and have intermittent on/off behavior.¹⁴ Moreover, quantum dots are generally incompatible with aqueous environments.^{5,15} These fluorescent reporters also require nearly continuous excitation, which leads to an increase in the background from scattered excitation light as well as autofluorescence, and greatly complicates the optical components required to read them.⁷ To reduce the background autofluorescence and the cost of the reader by eliminating advanced optical components, time-gated measurements were introduced using long-lived fluorescent reporters such as lanthanide-chelates.¹⁶ They have a longer emission lifetime than typical fluorescent reporters and therefore, a short time delay can be introduced between the excitation and measurement for the decay of the background signal. Although functional, these molecules tend to have photostability issues and therefore the time delay needs to be carefully defined, or the sensitivity can be greatly reduced when involved in time-gated measurements.⁷

To overcome many of these problems, we recently introduced persistent luminescent nanophosphors (PLNPs) as reporters for the LFA.^{7,17} In the last decade, PLNPs have gained great attention in biomedical applications such as bioimaging and photothermal therapies, owing to their unique optical characteristics.^{18,19} PLNPs generate a photon emission lasting for several minutes to hours after photoexcitation, vastly longer than the nanosecond lifetime of most fluorescent materials, allowing separation of emission signal from excitation light

by time-gated measurements.^{7,20} PLNPs also show excellent photostability.⁷ The combination of these properties allowed us to demonstrate a highly sensitive LFA for the detection of model protein hCG (human chorionic gonadotropin; LOD \approx 0.05 ng mL⁻¹) using a green-emitting SrAl₂O₄:Eu²⁺,Dy³⁺ (SAO) PLNP that could be detected and analyzed using smartphone-based time-gated imaging.^{17,21} SAO PLNPs were briefly excited with the phone's flash, followed by switching off the flash and collecting the emitted luminescence on the test and control lines with the smartphone's camera.¹⁷

Even with the resounding success of this initial demonstration, many practical limitations of this test would best be addressed by the creation of a multiplex LFA, which can save time and costs and improve diagnostic precision.^{22,23} Multiplex LFAs have been reported with different types of reporters, including gold nanoparticles,²⁴ colored latex beads,²⁵ fluorophores,²⁶ and quantum dots.^{27,28} Yet, these multiplex LFAs have the same limitations of sensitivity and reliability owing to the drawbacks of these reporters, as described above. In this study, we developed a new approach for a highly sensitive multiplex LFA using multiple PLNPs emitting at different wavelengths and coupled it with smartphone-based time-gated imaging. Our recent research suggested the best options for two PLNPs are the blue-emitting (Sr_{0.625}Ba_{0.375})₂MgSi₂O₇:Eu²⁺,Dy³⁺ (SBMSO) PLNPs, which can be detected using the smartphone-based imaging as well as our previously used SAO PLNPs.^{20,29} Therefore, as illustrated in Fig. 1, SAO and SBMSO compounds were used in tandem as reporters to build a novel smartphone-based multiplexed LFA that can simultaneously detect two model analytes; prostate-specific antigen (PSA) and human chorionic gonadotropin (hCG) for which commercial high-affinity antibodies exist.

Employing two different phosphors emitting at different wavelengths is especially important to analyze a sample with antibodies that are not specific to a particular pathogen. Most multiplex tests rely on spatial multiplexing, where the analytes are captured on two or more test lines using the same optical reporter. However, if there is significant non-specific binding, the test can produce erroneous results. Associating a different color with each pathogen and subsequently analyzing the composition of the test region color would be a more robust approach to examine samples containing several antibodies that are not pathogen-specific. This has been investigated previously using colored latex beads²⁵ and silver nanoparticles³⁰ as reporters. Although these results are encouraging, the colorimetric optical reporters may limit the test's sensitivity. In this work, we have used multiple PLNPs as reporters to achieve a highly sensitive and reliable LFA as a versatile multiplex point-of-need test for the quantitative detection of multiple analytes simultaneously.

2. Experimental section

2.1 Nanophosphor preparation, milling, and fractionation

SrAl₂O₄:Eu²⁺,Dy³⁺ (SAO) was purchased from Glow Inc. and the starting particle size (d_{50} = 5–15 μ m) was reduced by dispersing 10 g of powder in 100 mL of anhydrous ethanol (Decon) and ball milling for 10 days in a ceramic milling jar with zirconia grinding media.⁷ The powder was then dried and phase purity of the milled particles was confirmed with a PANalytical X'Pert powder diffractometer using Cu K α radiation (1.54183 Å).

Polycrystalline powder with the nominal composition $[(\text{Sr}_{0.625}\text{Ba}_{0.375})_{1.96}\text{Eu}_{0.01}\text{Dy}_{0.03}]\text{MgSi}_2\text{O}_7$ (SBMSO) was prepared *via* high-temperature solid-state synthesis using SrCO_3 (98%; Alfa Aesar), BaCO_3 (98%; Johnson Matthey), MgO (99.99%; Sigma-Aldrich), SiO_2 (99.5%; Sigma-Aldrich), Eu_2O_3 (99.9%; Materion Advanced Chemicals), and Dy_2O_3 (99.99%; Sigma-Aldrich). As a flux, 5 wt% H_3BO_3 (99.98%; Sigma-Aldrich) was added. The reagents were hand-ground in an agate mortar and pestle for 30 min and then placed in a shaker mill (Spex 8000) for 45 min. The mixture was pressed into a pellet and heated at 1150°C for 6 h in a reducing atmosphere of 5% $\text{H}_2/95\%$ N_2 with heating and cooling rates of 3°C min^{-1} . The powder was then reground and sintered again at 1000°C for 4h with the same reducing atmosphere and ramp rates as the initial heating. The particle size of the product was reduced by ball milling in anhydrous ethanol for 10 days in a ceramic milling jar with zirconia grinding media. The powder was dried and phase purity of the final product was confirmed using a PANalytical X'Pert powder diffractometer using Cu K α radiation (1.54183 \AA).²⁰

The particle size distribution of the dry, ball-milled SAO and SBMSO particles was then reduced by differential centrifugal sedimentation (Beckman Coulter Avanti J-E centrifuge) using anhydrous ethanol as the solvent to separate the smaller particles.⁷

2.2 Silica encapsulation

A volume of 1 mL of fractionated PLNPs (2 mg mL^{-1}) was pipetted into a 2 mL microcentrifuge tube. In a different tube, a solution was prepared by adding $221.6 \mu\text{L}$ of anhydrous ethanol and $246.7 \mu\text{L}$ of DI water (Millipore Milli-Q), then adding $6.7 \mu\text{L}$ of tetraethyl orthosilicate (TEOS; 99%; Sigma-Aldrich). The mixture was added to the tube with the PLNPs, and it was placed in a bath sonicator (Fisher Scientific FS30) for 5 min. A volume of $25 \mu\text{L}$ of aqueous ammonium hydroxide (28–30%; Sigma-Aldrich) was added to the suspension, followed by sonication for another 30 min. The tube with nanophosphors was placed on a room temperature rotator for 7.5 hours. Finally, the particles were washed 3 times by adding 1 mL of anhydrous ethanol and using the centrifuge (Eppendorf Centrifuge 5418), to settle particles and remove the supernatant. The PLNPs were sonicated and vortexed thoroughly during the washings to minimize the formation of aggregates.⁷

The particle size of the bare and encapsulated nanophosphors was determined by observing the particles dispersed in ethanol under a transmission electron microscope (TEM; JEM-2010F) and the colloidal stability of the silica encapsulated nanophosphors was confirmed by measuring the zeta potential of particles dispersed in ethanol using a Zetasizer (Malvern).

2.3 Functionalization of nanophosphors with antibodies

For silanization, 1 mL of silica-encapsulated PLNPs in ethanol (2 mg mL^{-1}) were transferred into a 2 mL microcentrifuge tube. The solution was centrifuged for 3 min at 3000 rcf and the top $216 \mu\text{L}$ of ethanol was removed and discarded. A second solution was prepared by adding $155 \mu\text{L}$ of TEOS, $5 \mu\text{L}$ of triethoxysilylbutyraldehyde (TESBA; Gelest), and 1393 mL of anhydrous ethanol. 10 mL of this solution was added to the nanophosphors resuspended in ethanol. Another solution was prepared by adding 189 mL of DI water and

16.7 μL of aqueous ammonium hydroxide and this solution was also added to the nanophosphor suspension. The mixture was sonicated for 10 min in bath sonicator and then placed on room temperature rotator at 20 rpm for 12 hours. Finally, the PLNPs were washed with 1 mL of anhydrous ethanol at least 3 times. In each wash, particles were centrifuged at 3000 rcf for 3 min to remove as much supernatant as possible.

Following silanization, the PLNPs were washed once with DI water and once with phosphate buffered saline, pH 8 (PBS; Takara Bio) to prepare them for bioconjugation. The nanoparticles were re-suspended in 700 μL of PBS, pH 8 and sonicated for 5 min. 50 μg (50 μL of 1 mg mL^{-1} stock solution) of mouse monoclonal anti- β hCG antibodies (ABBCG-0402; Arista) or mouse monoclonal anti-PSA antibodies ([8301] ab403; abcam) were then added to the PLNP suspension and mixed by vortexing. A solution of 1 M NaBH_3CN (Thermo Scientific) in PBS, pH 8 was prepared, and 250 μL of that solution was added to the nanophosphor suspension. This combination was sonicated for 5 min and then placed on a rotator at 20 rpm for 2 hours at room temperature.

Finally, the PLNPs were washed once with PBS, pH 7.4 to prepare them for passivation. The particles were re-suspended in 200 μL of PBS. A solution of 40 mg mL^{-1} bovine serum albumin (BSA; 98%; Sigma-Aldrich) in PBS, pH 7.4 was prepared, and 750 μL was added to the nanophosphors. A volume of 50 μL of 1 M NaBH_3CN was also added to the nanophosphor suspension. After 5 min of sonication, the nanophosphors were placed on a room temperature rotator for 3 hours at 20 rpm followed by washing 3 times with PBS, pH 7.4. The particles were subsequently resuspended in 100 μL of borate storage buffer (10 mM sodium borate (J.T. Baker), 150 mM NaCl (Macron), 0.1% BSA, 0.04% 40 000 avg. mol. wt polyvinylpyrrolidone (PVP-40; Sigma-Aldrich), 0.025% Tween 20 (Sigma-Aldrich), pH 8.5) and stored in a 4 $^{\circ}\text{C}$ refrigerator.

2.4 Constructing LFA strips

Whatman FF80HP nitrocellulose membrane (GE Healthcare) was assembled on an adhesive backing card (MIBA-020; DCN Diagnostics) with Whatman standard 14 sample pad and Whatman CF 5 absorbent pad. The conjugate pad was not used since these lateral flow assays were run only for the experimental purpose. To prepare the LFA strips for the hCG assay, goat polyclonal anti- α hCG antibodies (ABACG-0500; Arista) and goat polyclonal anti-mouse IgG (ABGAM-0500; Arista) were diluted from the stock solution to 1 mg mL^{-1} in PBS for the test line and control line, respectively. These antibodies were striped on the nitrocellulose membrane using a BioDot dispenser (XYZ30600124) at a rate of 1 $\mu\text{L cm}^{-1}$. The striped membrane was dried at 37 $^{\circ}\text{C}$ for 30 minutes in an incubator (Robbins Scientific Micro Hybridization Incubator 2000) and then cut into 3 mm wide strips using a ZQ2000 Guillotine Cutter. For the assays including PSA, on the same 3 mm wide LFA test strips, goat polyclonal anti-PSA antibodies (AF1344; R&D systems; 1 μL of 0.3 mg mL^{-1}) and goat polyclonal anti-mouse IgG (1 μL of 0.3 mg mL^{-1}) were spotted manually since we did not have enough amount of concentrated antibodies to make strips using the BioDot, as PSA antibodies are expensive. The antibody-spotted strips were then dried at 37 $^{\circ}\text{C}$ for 30 minutes in an incubator.

2.5 Smartphone-based imaging of nanophosphors

An iPhone 5S and a 3-D printed attachment were used for the smartphone-based imaging. The 3-D printed attachment was designed to hold a lateral flow assay cartridge (part number MICA-125; DCN Diagnostics), such that the result window of the cartridge is aligned with the rear camera of the iPhone and occupying most of the field of view when the cartridge is fully inserted into the attachment. A proprietary software application called 'Luminostics' was used to control the flash and the rear camera of the iPhone. The flash excites the nanophosphors for ~3 s, and after switching off the flash the camera captures the images after ~100 ms time delay. The camera settings used were ISO 2000 and a 0.5 s exposure time. The camera captures four images and gives the average result.¹⁷ Each test was run in triplicate to confirm the reliability of the test and imaging software.

3. Results and discussion

3.1 Nanophosphor reporters

LFAs require nanoparticles to effectively flow through membranes with pore sizes ranging from less than one micrometer to a few micrometers. The commercially purchased powder and bulk synthesized powder both initially consist of large particles of about 10–15 μm .⁷ Therefore, milling and fractionation by differential centrifugal sedimentation of inorganic phosphors are necessary for reducing the particle size to the nano-scale. Small particle size also minimizes gravitational sedimentation and increases the surface-area-to-volume ratio to maximize the capacity for the conjugation of antibodies.^{7,31} After the fractionation of the particles from the bulk powder, the TEM images of the bare particles are shown in Fig. 2a and b. The particle size of SAO and SBMSO are ~200 nm and ~250 nm, respectively.

One limitation of PLNPs is that SAO nanoparticles, in particular, are sensitive to aqueous environments and will decompose with any prolonged exposure to water. However, the water stability of the nanophosphors is greatly improved by encapsulating the particles in a silica shell. A modified Stöber process was used here for the silica encapsulation of the particles, and the TEM images of encapsulated particles confirm the formation of a silica shell around the particle (Fig. 2c and d). This also enables the later reaction with trialkoxysilanes, which is a popular method to introduce reactive groups on silica/glass surfaces.⁷ After the silica encapsulation, the zeta potential was measured to confirm the colloidal stability. Zeta potential is caused by the surface charge and the magnitude of zeta potential indicates the degree of electrostatic repulsions between the particles in a dispersion. Therefore, a greater zeta potential usually prevents aggregation and hence correlates to the colloidal stability of the nanoparticles. Generally, colloids of a zeta potential greater than ± 30 mV are considered as stable.³² The zeta potential of silica encapsulated SAO and SBMSO were -37 mV and -48 mV, respectively, indicating good colloidal stability after silica encapsulation.

Functionalizing the PLNPs with antibodies then required reacting the silica-encapsulated nanophosphors with triethoxysilylbutyraldehyde (TESBA) to introduce surface aldehydes that react with primary amines on the antibodies to form stable secondary amine bonds under reductive amination conditions in the presence of sodium cyanoborohydride. Finally,

bovine serum albumin (BSA) was added to block any unreacted aldehyde sites to reduce non-specific binding.^{7,17}

X-ray photoelectron spectroscopy (XPS) was employed to confirm functionalization at each stage of the process. As shown in Fig. 3a (top), the spectrum of the ball milled (unencapsulated) SAO shows the Sr 3s, Sr 3p, Sr 3d peaks reside at 357.7 eV, 269.7 eV, and 134.5 eV whereas the Al 2s and Al 2p peaks are at 119.3 eV and 74.5 eV, respectively. No other signals were detected except for C, which likely stems from impurities and/or surface contamination. The spectrum of SAO encapsulated with silica in Fig. 3a (middle) shows prominent Si 2s and Si 2p peaks at 156.8 eV and 105.6 eV, respectively, while the Sr and Al peaks are significantly reduced indicating the particles are fully encapsulated with silica. Finally, the spectrum of SAO after functionalization with the antibodies in Fig. 3a (bottom) shows the presence of the N 1s peak at 404 eV, indicating the presence of a protein on the surface of the nanophosphors.⁷ In the same manner, the spectrum of milled bare SBMSO in Fig. 3b (top) shows Sr 3p, Sr 3d, Ba 4d peaks at 270.1, 134.9 eV and 90.1 eV, respectively, two Mg KLL peaks at 306.9 eV and 353.3 eV, and peaks at 153.3 eV (Si 2s) and 102.9 eV (Si 2p). The spectrum of SBMSO encapsulated with silica in Fig. 3b (middle) again shows prominent Si 2s, and Si 2p peaks at 155.0 and 103.8 eV, respectively, with the Sr, Ba, and Mg peaks all significantly reduced, indicating that these particles also are encapsulated with silica. Finally, the spectrum of antibody-functionalized SBMSO in Fig. 3b (bottom) shows N 1s peak at 398.7 eV, signifying the conjugation of a protein to the surface of the nanophosphors.³³ These results confirm that the PLNPs are encapsulated with silica and the antibodies are successfully conjugated to the nanophosphors.^{7,33}

3.2 Applying functionalized multicolor nanophosphors in an LFA format

The assay buffer and the particle concentration were optimized to minimize non-specific binding and optimize detection limits. The contents of all four buffers created are provided in the ESI.[†] The optimal assay buffer (buffer D) selected based on the least non-specific binding and brightest test result line contains 50 mM NaCl, 0.1% Tween 20, 10 mM Tris HCl, 0.25% PVP-40, and 0.1% BSA (pH = 8). The SAO and SBMSO particle concentrations were also optimized and found to be 0.13 mg mL⁻¹ and 1 mg mL⁻¹, respectively. Two model analytes (hCG and PSA) were thereafter used to test the possibility of using SAO and SBMSO particles as different reporters in a multiplex LFA for the detection of two different analytes simultaneously. The analyte and antibody-conjugated SAO and SBMSO complexes were first independently tested for binding with anti-hCG antibodies and anti-PSA antibodies on LFA strips under the optimum conditions. The samples were prepared by spiking the analyte into the buffer solution. The positive samples contain the analyte, and negative samples contain distilled water instead of the analyte. To run the assays, 40 µL of buffer solution consisting of nanophosphors (diluted to the optimized concentration) and 10 ng mL⁻¹ of the desired analyte was added onto the sample pad of each strip. The strips were then allowed to run for 20 minutes and then imaged using the Alpha Innotech FluorChem gel documentation system. Each test was run in triplicate to confirm the reliability of the test. As shown in Fig. 4, the complexes of analyte and

[†]Electronic supplementary information (ESI) available. See DOI: [10.1039/c9ay02247c](https://doi.org/10.1039/c9ay02247c)

antibody-conjugated SAO or SBMSO nanophosphors bind well with both anti-hCG antibodies and anti-PSA antibodies on the test line with minimum non-specific binding, in the individual assays proving both PLNPs can be used as optical reporters.

3.3 Point-of-need smartphone-based imaging of nanophosphors

The FluorChem images display bright signals from the LFA strips with nanophosphors; however, the images are mono-chromatic. Taking advantage of the different emission colors allows significant differentiation of the two reporters beyond only spatial resolution. The tests were therefore imaged using the camera on an iPhone 5S smartphone that is coupled to the LFA through a custom-designed attachment and 'Luminostics' application that operates the phone's LED flash as an excitation source for the nanophosphors and the camera for image capturing.¹⁷ This testing format is a significant advantage as a point-of-need test considering the ubiquitous availability and compact nature of the smartphone and LFA and also the low cost (\approx \$5 USD) and the simplicity of the design of the 3D-printable smartphone attachment.¹⁷ The PLNPs can both be excited by the phone's flash with SAO emitting a green photon ($\lambda_{\text{max}} \approx 520 \text{ nm}$)³¹ and SBMSO emitting a blue photon ($\lambda_{\text{max}} \approx 460 \text{ nm}$).²⁰ The app to operate the flash and camera employs time-gated imaging to decrease the background signal by introducing a 100 ms time delay that allows the LED light to decay before image capture. SAO and SBMSO were successfully imaged in this smartphone-based time-gated imaging system owing to their long emission lifetimes,^{17,20} as shown in Fig. 5. Therefore, this system could lead to a rapid, low cost, and reliable multiplex diagnostic test that will enable individuals to monitor their health anytime, anywhere.

The detection limits of PSA using SAO particles and hCG using SBMSO particles were determined by varying the concentration of each antigen from 0.02–10 ng mL⁻¹ and calculating the ratio of the test line intensity (TL) to the control line intensity (CL). To calculate the TL : CL ratio, the intensities of TL and CL were measured using ImageJ, and the background was subtracted to correct any non-specific adsorption. The tests were run in triplicate and the average intensity ratio of TL : CL and the associated standard deviation were determined, as shown in Fig. 6. The results indicate the detection limits of 0.1 ng mL⁻¹ of PSA with SAO and 1 ng mL⁻¹ of hCG with SBMSO. The detection limit of previously reported serum PSA lateral flow assays is around 0.3–0.8 ng mL⁻¹.^{34–36} The analytical sensitivities of the commercially available hCG lateral flow tests vary with most of the urine-based tests having detection limits around 2.25 ng mL⁻¹,^{37,38} according to the WHO 4th International Standard, and the most sensitive tests having detection limits between 0.5–0.9 ng mL⁻¹.^{17,38,39} Therefore, the detection limits of this minimally-optimized smartphone-based LFA for PSA and hCG are already competitive with commercially available tests.

3.4 Developing multi-line spatially-resolved and single-line spectrally-resolved multicolor duplex assays

To develop a multiplex assay, hCG and PSA proteins were used as model analytes. Even though these model proteins do not occur together in biological samples, there are commercially available high-affinity antibodies that allowed us to show the ability of the high sensitivity detection of nanophosphor reporters. In addition, since hCG and PSA have been commonly used in previous LFA studies, we would be able to compare our limit of

detection (LOD) with previously reported values for different types of reporters to prove the high sensitivity detection of nanophosphor reporters.

Specific binding of the complexes of analyte and antibody-conjugated nanophosphors to the desired antibodies on the LFA strips in the presence of other analytes and antibodies is a critical factor in developing a multiplex assay format. To examine the capability of specific binding, LFAs were first constructed that contain two test regions and one control region on the same membrane, as illustrated in Fig. 7a. The strips have anti-PSA and anti-hCG antibodies spotted at the first and second test region, respectively (Fig. 7b and c), and anti-mouse antibodies spotted at the control region. A solution of PLNPs functionalized with anti-hCG antibodies was then added to the sample pad along with hCG, and the results show that it is possible for SAO and SBMSO functionalized with anti-hCG antibodies to flow past the first spot with anti-PSA antibodies and form a bright positive band at the second spot where anti-hCG antibodies are located. In Fig. 7d and e, anti-hCG antibodies are placed in the first spot and anti-PSA antibodies are placed in the second spot. A solution containing PLNPs functionalized with anti-PSA antibodies and PSA antigen was added onto the sample pad. In this case, anti-PSA conjugated SAO and SBMSO flow through the first spot and formed a positive band at the second spot. Each test was run in triplicate to confirm the reliability of the test. In all cases, binding is only observed at the desired test region, and, most importantly, there is virtually zero-non-specific binding, indicating that the antibody-conjugated nanophosphors can bind specifically in the presence of multiple different analytes and antibodies.

The specific binding ability of antibody conjugated SAO and SBMSO allows developing a multiplex assay to detect multiple analytes simultaneously. Therefore, a spatial duplex assay was developed using SAO conjugated to anti-PSA antibodies and SBMSO conjugated to anti-hCG antibodies to detect a solution containing a dilute mixture of PSA and hCG antigens. Spatially-resolved multiplex assays differentiate analytes by physically separating the detections sites.^{40,41} As illustrated in Fig. 8, two test regions were placed on the nitrocellulose membrane by spotting polyclonal anti-PSA antibodies (spot 1) and polyclonal anti-hCG antibodies (spot 2). Anti-mouse antibodies were spotted in the control region. A solution containing 0.13 mg mL^{-1} SAO functionalized with monoclonal anti-PSA antibodies and 10 ng mL^{-1} PSA in the optimized assay buffer was prepared. A second solution containing 1 mg mL^{-1} SBMSO nanophosphors functionalized with monoclonal anti-hCG antibodies, and 10 ng mL^{-1} hCG in an optimized assay buffer was also prepared. $40 \text{ }\mu\text{L}$ of each solution was mixed in another microcentrifuge tube and then loaded onto the sample pad. The strip was allowed to run for 20 minutes, followed by washing with $80 \text{ }\mu\text{L}$ of assay buffer to remove unbound reporter particles. Finally, the LFA strip was imaged using the iPhone 5S, and the data are shown in Fig. 8. It is clear that the SAO particles are localized at the first test region containing anti-PSA antibodies, as indicated by the green band, and SBMSO particles are only bound at the second test region containing anti-hCG antibodies, as shown by the blue band. The control region is blue-green because both SAO and SBMSO particles bind with the anti-mouse antibodies in the control region. These results prove that these two compounds can be successfully used for the simultaneous detection of two different analytes in the same sample with minimal non-specific binding and that the two emission signals can be detected at the same time.

With the ability to discriminate the analytes based on spatial separation as well as the color of the reporter, the multiplex assay was performed varying the concentration of one analyte while maintaining the concentration of the other analyte constant at its detection limit to confirm the detection limits of the assay in a multiplex format. First, the detection limit of PSA in the multiplex assay was tested by varying the PSA concentration from 0.02–10 ng mL⁻¹ in the presence of a constant concentration of 1 ng mL⁻¹ of hCG. The calculated intensity ratios of test spot 1/control spot are shown in Fig. 9a. The detection limit cutoff, which is the mean plus three times the standard deviation ($\mu + 3\sigma$) of the no-analyte controls, is marked by the red horizontal line. Based on this analysis, shown in Fig. 9a, the detection limit is found to be 0.1 ng mL⁻¹, which is in agreement with the previous result of SAO in the single-plex format. The blue line shows the intensity ratio of test spot 2/control spot at the constant concentration of 1 ng mL⁻¹ hCG, and it remains nearly constant at different concentrations of PSA. Next, to find the detection limit of hCG in the multiplex format, a concentration series from 0.02–10 ng mL⁻¹ of hCG was used in the presence of a constant concentration of 0.1 ng mL⁻¹ of PSA. The calculated intensity ratios of test spot 2/control spot are shown in Fig. 9b. In this case, the detection limit is 1 ng mL⁻¹ of hCG. The green line shows the intensity ratio of test spot 1/control spot at the constant concentration of 0.1 ng mL⁻¹ PSA, and it also remains nearly constant at different hCG concentrations. These results indicate that the multiplex format does not change the detection limits found in the individual assays. Moreover, the intensity ratio of the test region/control region for the target analyte is independent of the concentration of the other analyte. SAO and SBMSO in conjugation with the point-of-need smartphone testing platform can, therefore, be used for the highly sensitive, concurrent detection of two different analytes.

Although these LFA strips show excellent detection limits, any traditional reporter can be used in the multiplex formation using spatial separation of the test lines. One of the major advantages of using reporters that produce different optical signatures is the ability to also spectrally resolve their signal. Thus in a spectral multiplex assay, different analytes are detected on a single detection site using different color labels for each analyte.^{25,40} Therefore, the above system was also developed as a spectral duplex assay where both types of capture antibodies are spotted at the same test region. As illustrated in Fig. 10a, both polyclonal anti-PSA and polyclonal anti-hCG antibodies were spotted in the test region. Anti-mouse antibodies were spotted in the control region. A solution containing 0.13 mg mL⁻¹ SAO functionalized with monoclonal anti-PSA antibodies and 10 ng mL⁻¹ PSA in the optimized assay buffer was prepared. A second solution containing 1 mg mL⁻¹ SBMSO nanophosphors functionalized with monoclonal anti-hCG antibodies and 10 ng mL⁻¹ hCG in an optimized assay buffer was also prepared. 40 μ L of each solution was mixed, loaded onto the sample pad, and the strip was allowed to run for 20 minutes. It was then washed with 80 μ L of assay buffer. Finally, the LFA strip was imaged using the iPhone 5S platform. As shown in Fig. 10a, SAO and SBMSO particles are both captured at the test region, and the control region signified by the blue-green emission.

Decomposing the signal at the test region (Fig. 10b), by post-processing the image into the green color channel and blue color channel reveals the presence of both green and blue signatures that can be plotted to reveal a relative intensity of the two channels (Fig. 10c). This spectral assay is especially useful to analyze samples containing antibodies that are not

specific to a particular pathogen (*e.g.*, acute febrile illnesses).²⁵ In that case, two different colors can be associated with two different pathogens and by analyzing the color composition of the test region, the causative pathogen can be identified. Finally, the same spectral duplex assay was performed with different concentrations of PSA and hCG antigens as shown in Fig. 11a. The LFA strips were imaged on the iPhone 5S and the green and blue colors of the test region of each strip were separated and plotted in Fig. 11b as a function of antigen concentration. In this spectral multiplex format, minimal non-specific binding is observed in the no-analyte control. Nevertheless, for the remainder of the strips, when the signal is decomposed into the green and blue channels, the signal intensity of the no-analyte control is very low compared to the positive samples. As shown in Fig. 11b, the green and blue intensities increase with increasing concentrations of PSA and hCG, respectively. Therefore, this system is capable of quantitative detection of multiple analytes concurrently.

4. Conclusions

This work demonstrated a new multiplex LFA capable of detecting two analytes simultaneously using PLNPs as reporters. Wet milling is necessary to reduce the particle size of both nanophosphor reporters, and differential centrifugal sedimentation can be used to fractionate smaller particles. The water stability of particles was enhanced using a modified Stöber process to make a silica shell around the particles. Facile bioconjugation schemes such as reductive amination can subsequently link the antibodies onto the silica surface of the particle. The resulting antibody conjugated SAO and SBMSO can simultaneously detect PSA and hCG proteins giving more sensitive and reliable results than the other conventional reporters. More importantly, the long emission lifetime of PLNPs eliminates the need for continuous excitation, which is required for standard fluorescence measurements; there is a substantially lower background signal and no need for advanced optical hardware. Therefore, PLNPs can be imaged using a smartphone-based time-gated imaging system, which enables the development of a simple, fast and inexpensive point-of-need diagnostic method to detect analytes in color quickly. SAO and SBMSO PLNPs can be successfully detected whether they are bound on two different lines (spatially resolved) or at the same test region (spectrally resolved) to detect PSA and hCG concurrently. It is also possible to integrate the emission intensity independently and determine the ratio of the analytes contained within a sample. Therefore, this system shows outstanding potential for the future development of a highly sensitive, quantitative detection tool for multiple analytes.

Supplementary Material

Refer to Web version on PubMed Central for supplementary material.

Acknowledgements

The authors thank the Department of Chemistry at the University of Houston for providing startup funds and NIH (Grant No. 1R01AR072742-01) and CDC (Grant No. 1U01CK000512-01) for funding this research. The authors also thank Dr Andrew Paterson and Dr Balakrishnan Raja, formerly in the RCW laboratory and now at Luminostics, Inc. for helping with the protocol for the functionalization of nanophosphors and providing the 'Luminostics' app for smartphone-based imaging. The authors also thank Heather Goux for training on LFA and Angelica Cobb for help in the synthesis of SBMSO and fractionation of particles.

References

1. Vashist SK, *Biosensors*, 2017, 7, 62.
2. Price CP, *Br. Med. J.*, 2001, 322, 1285–1288. [PubMed: 11375233]
3. Hu J, Wang S, Wang L, Li F, Pingguan-Murphy B, Lu TJ and Xu F, *Biosens. Bioelectron.*, 2014, 54, 585–597. [PubMed: 24333570]
4. Kozel TR and Burnham-Marusch AR, *J. Clin. Microbiol.*, 2017, 55, 2313–2320. [PubMed: 28539345]
5. Sajid M, Kawde A-N and Daud M, *J. Saudi Chem. Soc.*, 2015, 19, 689–705.
6. Koczula KM and Gallotta A, *Essays Biochem.*, 2016, 60, 111–120. [PubMed: 27365041]
7. Paterson AS, Raja B, Garvey G, Kolhatkar A, Hagstrom AE, Kourentzi K, Lee TR and Willson RC, *Anal. Chem.*, 2014, 86, 9481–9488. [PubMed: 25247754]
8. Wong RC and Tse HY, *Lateral Flow Immunoassay*, Humana Press, New York, 2009.
9. Zhang C, Zhang Y and Wang S, *J. Agric. Food Chem.*, 2006, 54, 2502–2507. [PubMed: 16569035]
10. Yang W, Li XB, Liu GW, Zhang BB, Zhang Y, Kong T, Tang JJ, Li DN and Wang Z, *Biosens. Bioelectron.*, 2011, 26, 3710–3713. [PubMed: 21377861]
11. Lee LG, Nordman ES, Johnson MD and Oldham MF, *Biosensors*, 2013, 3, 360–373. [PubMed: 25586412]
12. Foubert A, Beloglazova NV and De Saeger S, *Anal. Chim. Acta.*, 2017, 955, 48–57. [PubMed: 28088280]
13. Zheng Q, Jockusch S, Zhou Z and Blanchard SC, *Photochem. Photobiol.*, 2014, 90, 448–454. [PubMed: 24188468]
14. Mahler B, Spinicelli P, Buil S, Quelin X, Hermier JP and Dubertret B, *Nat. Mater.*, 2008, 7, 659–664. [PubMed: 18568030]
15. Walling MA, Novak JA and Shepard JR, *Int. J. Mol. Sci.*, 2009, 10, 441–491. [PubMed: 19333416]
16. Ye Z, Tan M, Wang G and Yuan J, *J. Mater. Chem.*, 2004, 14, 851–856.
17. Paterson AS, Raja B, Mandadi V, Townsend B, Lee M, Buell A, Vu B, Brgoch J and Willson RC, *Lab Chip*, 2017, 17, 1051–1059. [PubMed: 28154873]
18. Liu J, Lécuyer T, Seguin J, Mignet N, Scherman D, Viana B and Richard C, *Adv. Drug Delivery Rev.*, 2019, 138, 193–210.
19. Maldiney T, Richard C, Seguin J, Wattier N, Bessodes M and Scherman D, *ACS Nano*, 2011, 5, 854–862. [PubMed: 21291197]
20. Finley E, Cobb A, Duke A, Paterson A and Brgoch J, *ACS Appl. Mater. Interfaces*, 2016, 8, 26956–26963. [PubMed: 27635436]
21. Willson R and Paterson A, EP3036530A1, 2016.
22. Li J and Macdonald J, *Biosens. Bioelectron.*, 2016, 83, 177–192. [PubMed: 27125840]
23. Hanafiah KM, Arifin N, Bustami Y, Noordin R, Garcia M and Anderson D, *Diagnostics*, 2017, 7, 51.
24. Chen Y, Chen Q, Han M, Zhou J, Gong L, Niu Y, Zhang Y, He L and Zhang L, *Food Chem.*, 2016, 213, 478–484. [PubMed: 27451207]
25. Lee S, Mehta S and Erickson D, *Anal. Chem.*, 2016, 88, 8359–8363. [PubMed: 27490379]
26. Xu Y, Liu Y, Wu Y, Xia X, Liao Y and Li Q, *Anal. Chem.*, 2014, 86, 5611–5614. [PubMed: 24892496]
27. Wu F, Yuan H, Zhou C, Mao M, Liu Q, Shen H, Cen Y, Qin Z, Ma L and Li LS, *Biosens. Bioelectron.*, 2016, 77, 464–470. [PubMed: 26454828]
28. Taranova NA, Berlina AN, Zherdev AV and Dzantiev BB, *Biosens. Bioelectron.*, 2015, 63, 255–261. [PubMed: 25104435]
29. Brgoch J and Finley E, US Pat. 20180080874A1, 2016.
30. Yen C-W, de Puig H, Tam JO, Gomez-Marquez J, Bosch I, Hamad-Schifferli K and Gehrke L, *Lab Chip*, 2015, 15, 1638–1641. [PubMed: 25672590]
31. Finley E, Paterson AS, Cobb A, Willson RC and Brgoch J, *Opt. Mater. Express*, 2017, 7, 2597–2616.

32. Schierz A and Zanker H, *Environ. Pollut*, 2009, 157, 1088–1094. [PubMed: 19010575]
33. NIST X-ray Photoelectron Spectroscopy Database, <https://srdata.nist.gov/xps/Default.aspx>, accessed April 10, 2019.
34. Andreevaa IP, Grigorenkoa VG, Egorova AM and Osipov AP, *Anal. Lett*, 2016, 49, 579–588.
35. Li X, Li W, Yang Q, Gong X, Guo W, Dong C, Liu J, Xuan L and Chang J, *ACS Appl. Mater. Interfaces*, 2014, 6, 6406–6414. [PubMed: 24761826]
36. Barnett JM, Wraith P, Kiely J, Persad R, Hurley K, Hawkins P and Luxton R, *Biosensors*, 2014, 4, 204–220. [PubMed: 25587419]
37. Gnoth C and Johnson S, *Geburtshilfe Frauenheilkd*, 2014, 74, 661–669. [PubMed: 25100881]
38. Silva de Moraes G, Cristovam R and Savaris RF, *Rev. Assoc. Med. Bras*, 2011, 57, 506–512.
39. Cole LA, *Clin. Chem. Lab. Med*, 2011, 49, 1317–1322. [PubMed: 21812725]
40. Anfossi L, Nardo FD, Cavalera S, Giovannoli C and Baggiani C, *Biosensors*, 2019, 9(1), 2.
41. Boutal H, Vogel A, Bernabeu S, Devilliers K, Creton E, Cotellon G, Plaisance M, Oueslati S, Dortet L, Jousset A, Simon S, Naas T and Volland H, *J. Antimicrob. Chemother*, 2018, 73, 909–915. [PubMed: 29365094]

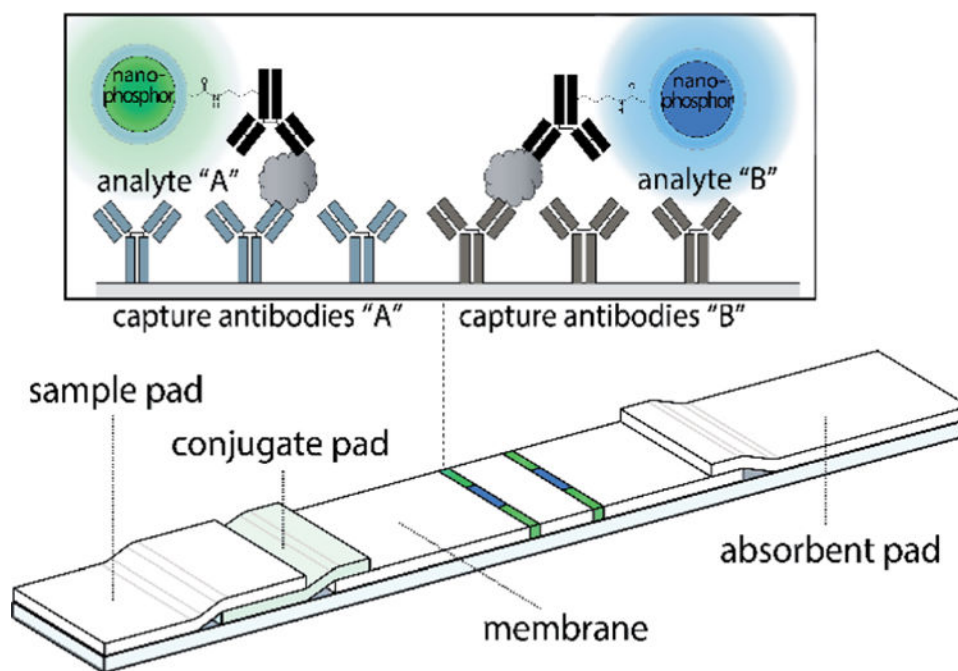


Fig. 1. Schematic representation of a duplex lateral flow assay where the green-emitting $\text{SrAl}_2\text{O}_4:\text{Eu}^{2+},\text{Dy}^{3+}$ (SAO) and blue-emitting $(\text{Sr}_{0.625}\text{Ba}_{0.375})_2\text{MgSi}_2\text{O}_7:\text{Eu}^{2+},\text{Dy}^{3+}$ (SBMSO) PLNPs are employed as reporters.

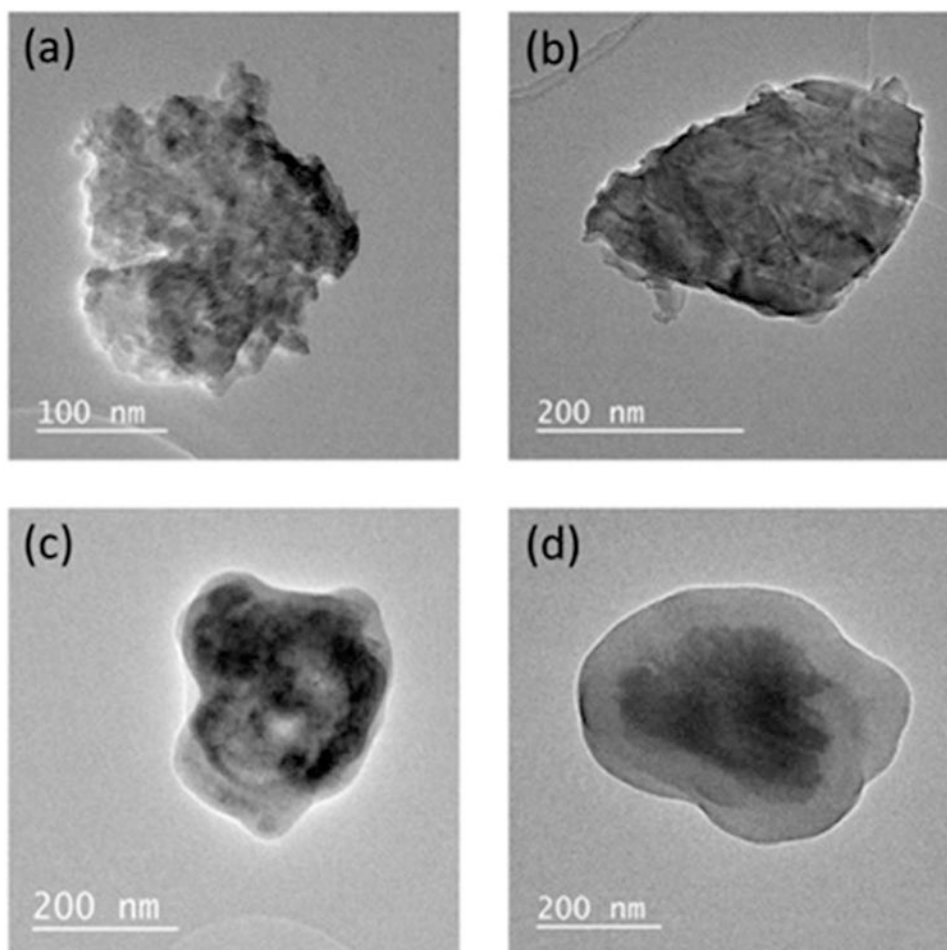


Fig. 2. Transmission Electron Microscope (TEM) images of (a) bare SAO (b) bare SBMSO (c) silica encapsulated SAO (d) silica encapsulated SBMSO.

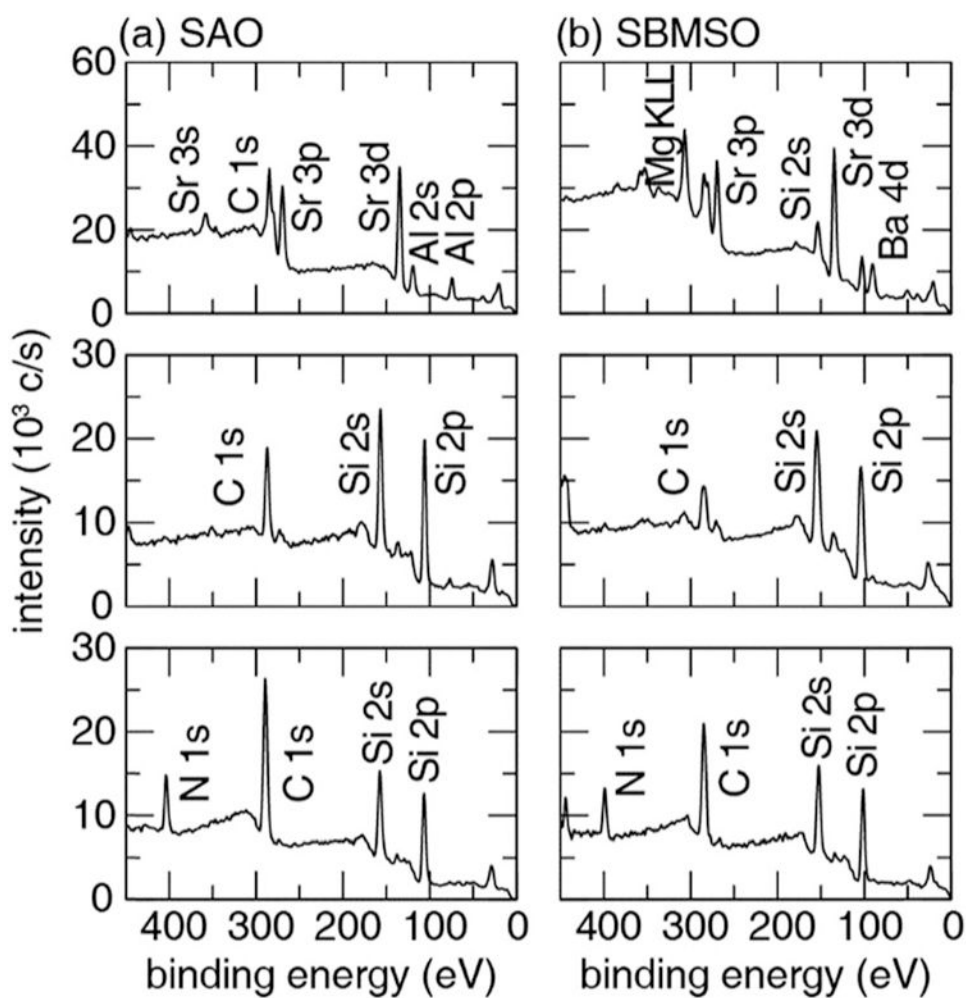


Fig. 3. XPS spectra of (a) SAO and (b) SBMSO at different stages of functionalization: (top) milled bare (middle) after silica encapsulation (bottom) after functionalization with antibodies.

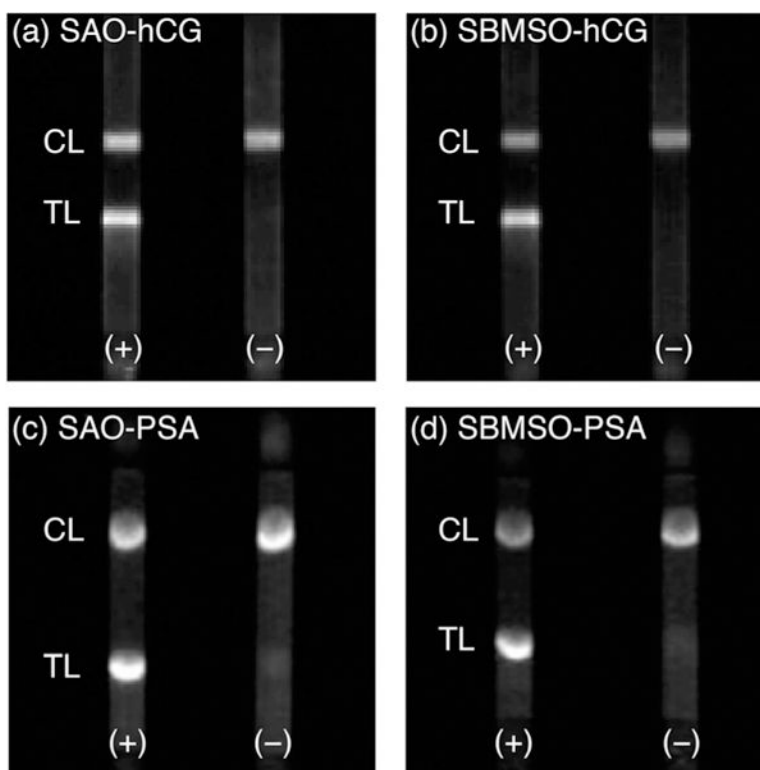


Fig. 4. Binding of (a) 0.13 mg mL^{-1} SAO in hCG assay, (b) 1 mg mL^{-1} SBMSO in hCG assay, (c) 0.13 mg mL^{-1} SAO in PSA assay, and (d) 1 mg mL^{-1} SBMSO in PSA assay using buffer D. These grayscale images were collected using the FluorChem gel documentation system.

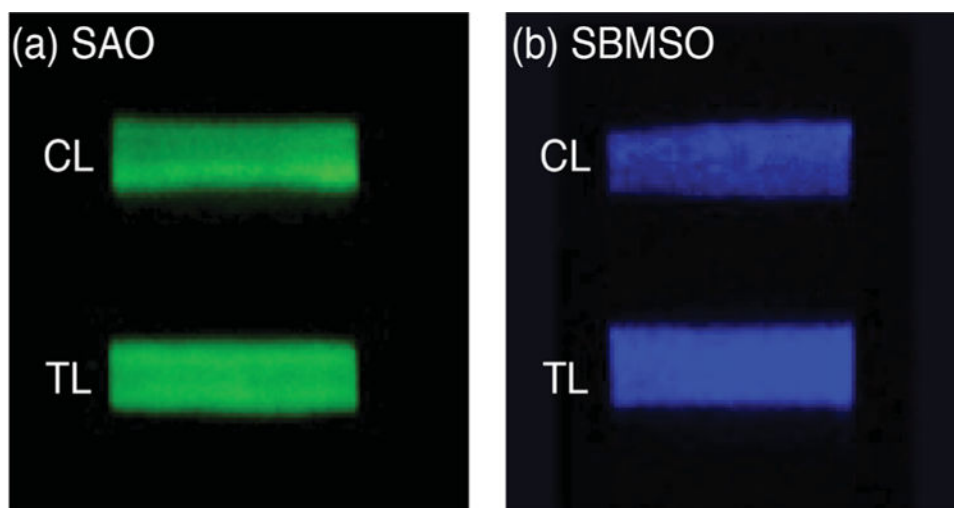


Fig. 5.
(a) SAO and (b) SBMSO detected on iPhone 5S. The color images were collected using an iPhone 5s rear camera.

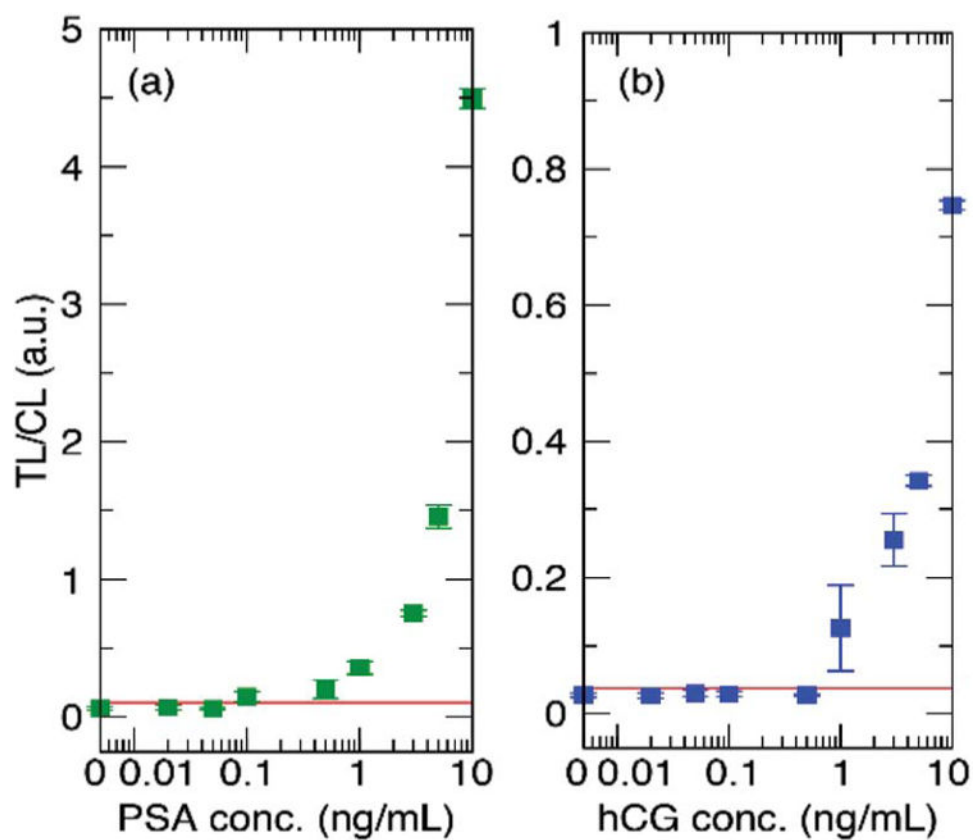


Fig. 6. Serial dilution of (a) PSA with SAO and (b) hCG with SBMSO detected on the iPhone 5S. The red line signifies the detection limit cutoff taken as the mean plus three times the standard deviation ($\mu + 3\sigma$) of the no-analyte control tests.

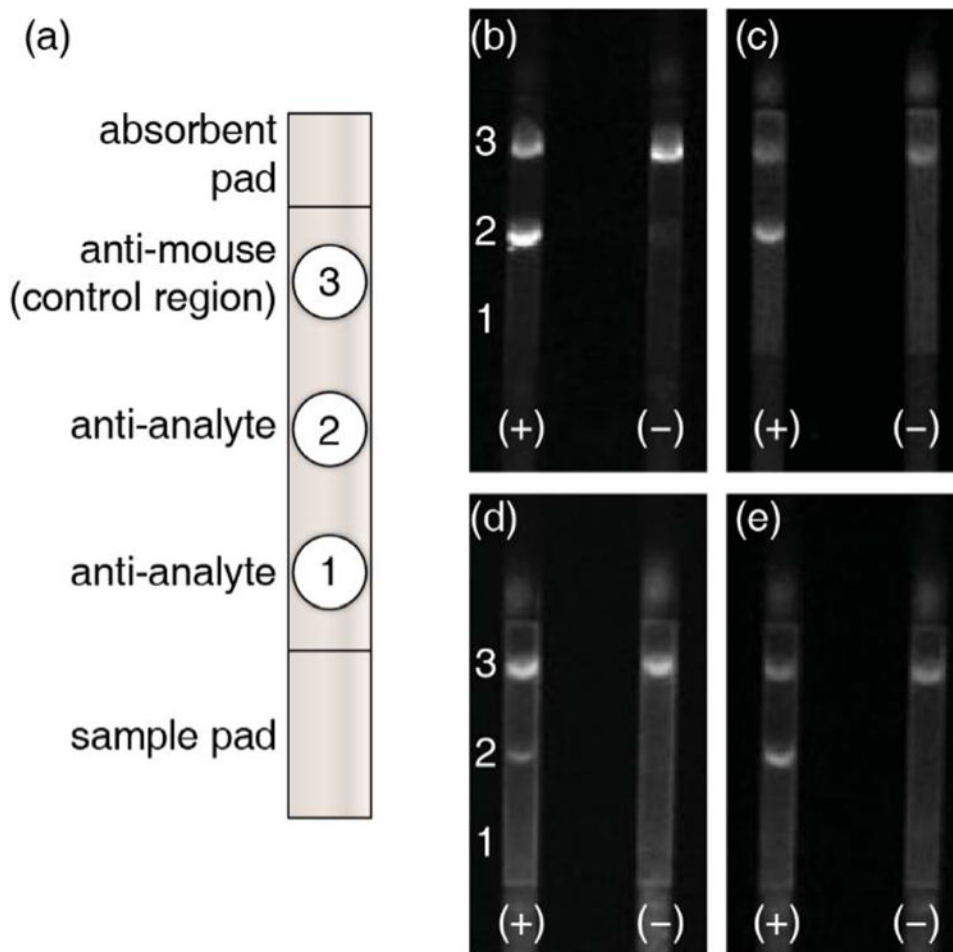


Fig. 7. (a) Schematic representation. Specific binding of (b) SAO with anti-hCG antibodies (c) SBMSO with anti-hCG antibodies (d) SAO with anti-PSA antibodies (e) SBMSO with anti-PSA antibodies. These grayscale images were collected using the FluorChem gel documentation system.

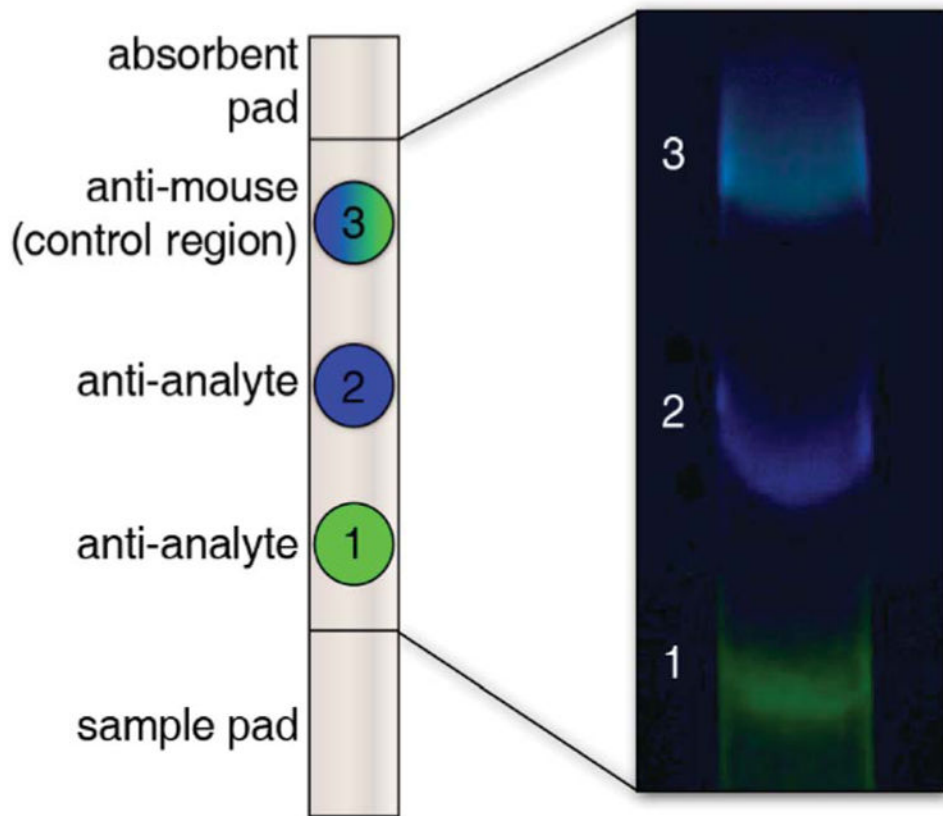


Fig. 8. Spatial duplex LFA using SAO for anti-PSA antibodies (green) on spot 1 and SBMSO for anti-hCG antibodies (blue) on spot 2 imaged in color using iPhone 5S. The control region is a mixture of SAO and SBSMO and therefore appears bluish-green.

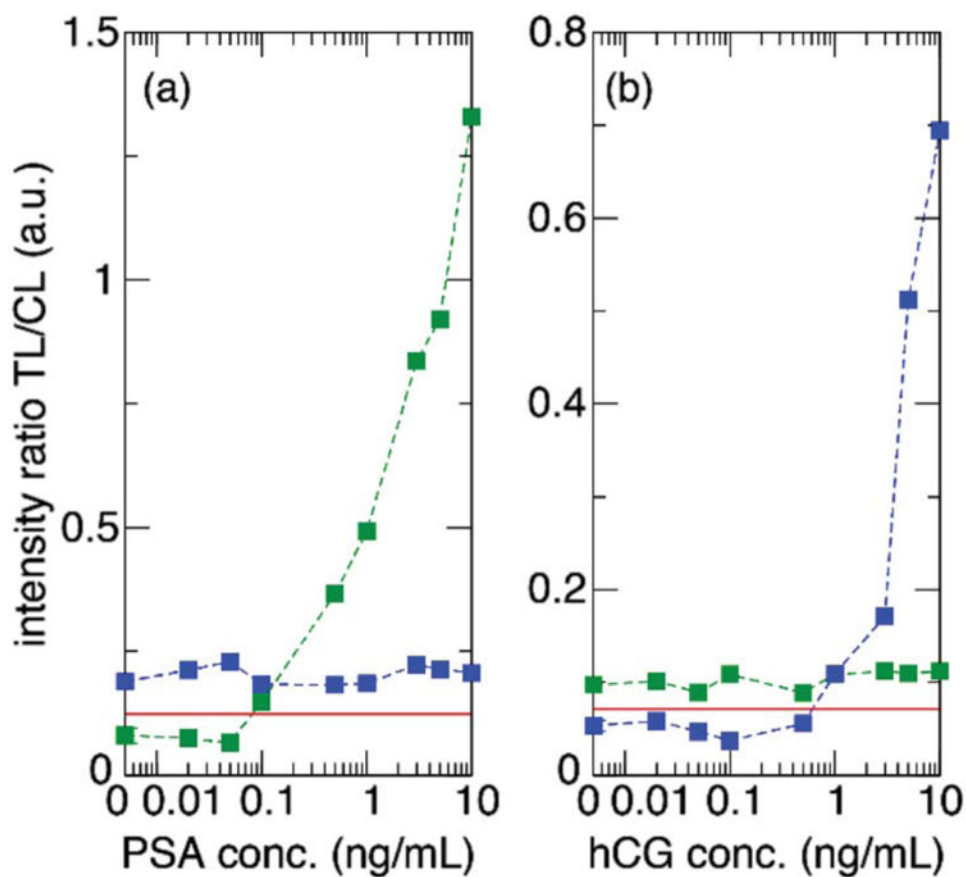


Fig. 9. Serial dilution of (a) PSA with SAO in the presence of 1 ng mL⁻¹ hCG and (b) hCG with SBMSO in the presence of 0.1 ng mL⁻¹ PSA detected on the iPhone 5S.

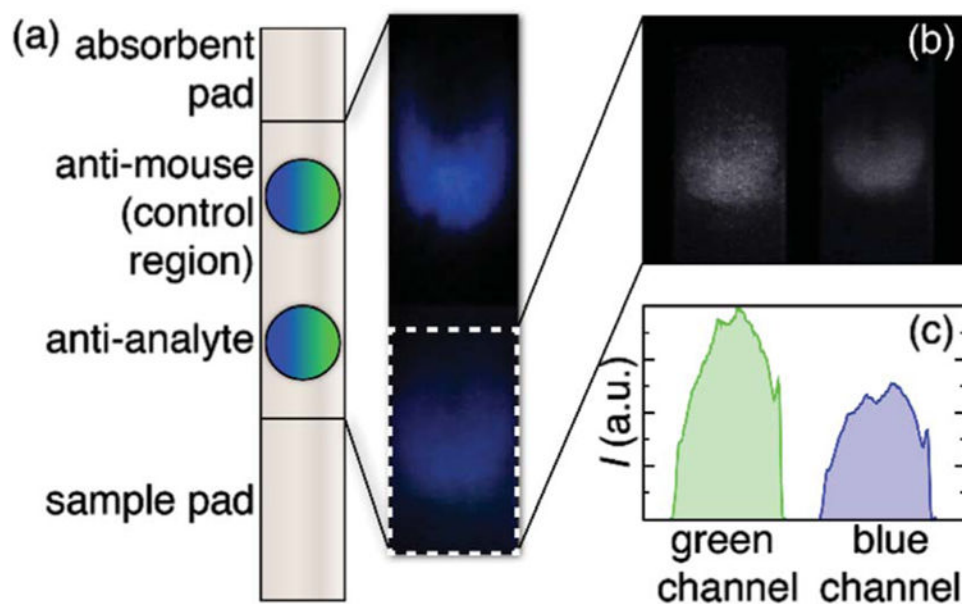


Fig. 10.

(a) Spectral duplex LFA using SAO conjugated to anti-PSA antibodies (green) and SBMSO conjugated to anti-hCG antibodies (blue) both binding at the test region in the presence of PSA and hCG analytes indicating a positive result. Decomposing the signal at the test region (b) reveals two distinct signals (c) that correspond to the green and blue color channels of the smartphone camera. These color images were collected and processed using the iPhone 5S and the associated application.

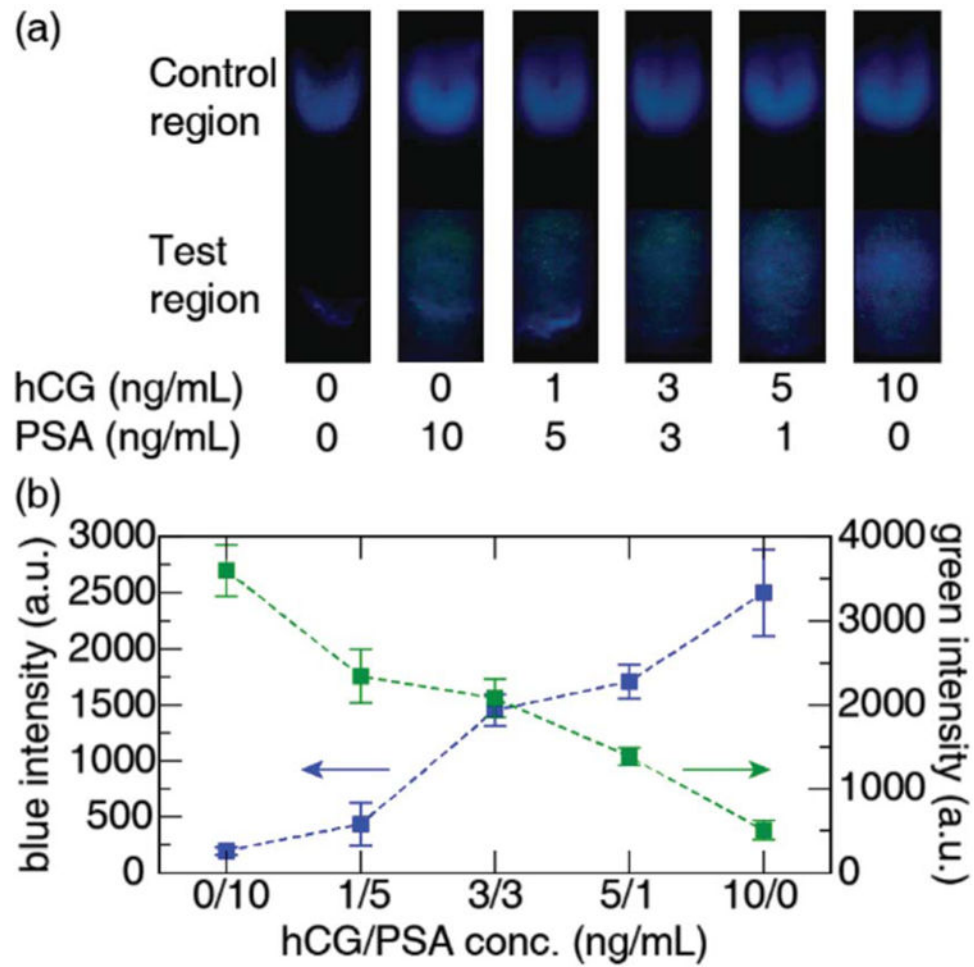


Fig. 11.

(a) iPhone images of LFA strips with varying concentrations of PSA and hCG. (b)

Intensities of green and blue channels of the test region with varying concentrations of PSA and hCG. The color images were collected using an iPhone 5s rear camera.